Iron Behavior in Microcosms Simulating Bioreduction in Savannah River Site Sediments- 17389

Yelena Katsenovich[a], Aref Shehadeh[a], Miles Denham[b]

[*]Applied Research Center, Florida International University,
10555 W. Flagler St., EC 2100, Miami, FL 33174
[**]Savannah River National Laboratory, Aiken, SC 29808

ABSTRACT

An estimated 1.8 billion gallons of acidic low-activity waste solutions originating from the processing of uranium slugs and irradiated fuel at separation facilities at the Savannah River Site (SRS) were discharged to the unlined seepage basins located in the F/H-area. The acidic solutions of the basin influent (pH from 3.2 to 5.5) contaminated with a variety of radionuclides and dissolved metals caused groundwater contamination. In 2010, DOE funded a demonstration of the Enhanced Anaerobic Reductive Precipitation (EARP) process at the SRS F-Area that consisted of *in-situ* injections of a carbohydrate substrate to establish anaerobic reactive zones for metal and radionuclide remediation. The addition of the molasses substrate solution to groundwater was done to produce anaerobic conditions conducive to uranium reduction and then precipitation as uranium (IV). The SRS soil is highly weathered and features very low natural alkalinity. A microcosm study, prepared with sieved SRS sediments and augmented with a solution mixture containing molasses and sulfate, was designed to provide evidence of the capabilities of this remediation technology under SRS environmental conditions. The objective of these microcosm experiments was to replicate the anaerobic conditions created as a result of injections of molasses combined with sulfate ions, similar to the EARP process that was performed at SRS, and investigate if any mineralogical changes could occur in the soil due to the addition of molasses. Specifically, the study aimed to determine if solid phases of reduced iron such as siderite and pyrite would be formed, as this would indicate the potential to form a long-lasting bioreductive zone. An understanding of this technology will be useful in determining if it is a viable option for remediation.

In the experiments, the media solution was amended with molasses and sulfate to stimulate sulfate-reducing bacteria. Sulfate reduction occurs extensively under the redox conditions occurring after iron reduction and before methanogenic conditions. These conditions are considered the second most reducing condition in natural groundwater systems. Microcosm tubes prepared in triplicate were kept inside an anaerobic glove box, which was continuously monitored to ensure that conditions remained anaerobic. The initial X-ray diffraction (XRD) analyses on the background sediment samples indicated the presence of quartz, kaolinite, montmorillonite, and goethite. In the molasses-treated samples there were no visible peaks for reduced forms of iron such as siderite and pyrite.

The pH measurements suggest that all samples in either batch, including those that were brought to a neutral pH before the addition of the sediments, have followed a similar trend with a decline in the pH value to between 4 and 4.7. This can be attributed to the fermentation of molasses and the natural acidity of the SRS

sediments used for the microcosm study. In the acidic iron-rich sediment, the microbial reduction of Fe (III) was the predominant electron-accepting process for oxidation of the organic substrate. The maximum iron concentration detected during the experiments was 13 mg/L. Analytical results showed that there was no sulfate reduction in any of the samples augmented with sulfate and the concentration remained level at 500 ppm as originally added to the initial solutions (518 - 542 mg/L). This is consistent with the absence of any indication of iron sulfide formation. Under the experimental conditions in these microcosms, the abundance of biologically available Fe (III) allows Fe (III)-reducers to outcompete sulfate-reducing bacteria using molasses as an electron donor.

INTRODUCTION

Enhanced *in situ* anaerobic bioremediation can be an effective means for the degradation and/or retardation of contaminants found in groundwater. Due to the fact that it is *in situ*, this process leaves little impact on site and facility operations and generates no waste. Because it relies on microorganisms already present in the soil, it is also relatively low-cost when compared to active engineered remediation. The enhanced anaerobic reductive precipitation (EARP) process is one of these bioremediation methods. EARP utilizes a carbohydrate-substrate such as whey, molasses or high fructose corn syrup, for example, to serve as an electron donor and drive down the oxidation-reduction potential of the groundwater to a more reduced state. By doing this, the reductive precipitation of dissolved metals and dissolved radionuclides into less reactive forms is likely to occur. This has been proven to be a useful way to control transport of contaminants via groundwater flows.

In 2010, ARCADIS demonstrated the use of *in situ* injections of a carbohydrate substrate, molasses, to create reactive zones for uranium (VI) remediation via the EARP process at the F- Area of the Savannah River Site (SRS) (Lutes et al., 2014). The addition of the molasses substrate solution to groundwater was done to produce anaerobic conditions conducive to uranium reduction and then precipitation as uranium (IV) (Dennis and Suthersan 1998). This remediation strategy relies on changing the geochemical conditions in a direction that is opposite the natural aerobic condition of the aquifer. The geochemical conditions will evolve back toward aerobic as oxic groundwater flows back into the treated site.

An important aspect of any *in situ* remediation technology for radionuclides is to prove the longevity of contaminant immobilization, particularly when remediation relies on establishing conditions that are not natural to the aquifer. After use of the EARP technology, contaminants may remain relatively immobile for a long period if they coprecipitate with a phase that is stable under aerobic conditions or if a sufficient mass of reduced iron minerals is created in the treatment zone to react with influxing dissolved oxygen for a long period of time.

In this study, we investigate the behavior of iron in sediments from the SRS aquifer under induced anaerobic conditions using microcosms. SRS soil is highly weathered with little buffering capacity. The sediments at the F-area are classified as weathered sands with very high quartz content with kaolinite, montmorillonite, and goethite present to a lesser degree (Dong et al. 2012b). A microcosm study prepared with sieved SRS sediments and augmenting the solution mixture with molasses, was designed to examine iron behavior during EARP remediation for SRS conditions. The

objective of these microcosm experiments was to replicate the anaerobic conditions created as a result of injections of molasses combined with sulfate ions similar to the EARP process that was performed at SRS and investigate if any mineralogical changes could occur in the soil due to the addition of molasses. Specifically, the study aimed to determine if forms of reduced iron such as siderite and pyrite would be created, as this would indicate that the EARP process had created the lasting bioreductive zone that was desired. An understanding of the iron behaviorwill be useful to determining if it is a viable option for remediation.

An important step in the EARP process is to deplete terminal electron acceptors until sulfate reducing conditions are achieved. Sulfate reduction occurs extensively in the redox conditions occurring after iron reduction and before methanogenic conditions at E_h^o= -220. These conditions are considered the second most reducing condition in natural groundwater systems. Sulfate reducing bacteria (SRB) are a very diverse group of obligatory anaerobes, which have an ability to dissimilate sulfate to sulfide while oxidizing various growth substrates (Willis et al. 1997). Molasses is one of the substrates that have been described as an electron donor and carbon source for the cultivation of SRB (Annachhatre and Suktrakoolvait 2001, Hussain et al. 2014).

Under environmental conditions, sulfate reduction, mediated exclusively by prokaryotic sulfate-reducing bacteria, results in chemical reactions in which the organic substrate is oxidized while sulfate is reduced (Eq.1) (Canfield 2001, Berner et al. 2002, Aravena and Mayer, 2009):

$$SO_4^{2-} + 2CH_2O \rightarrow H_2S + 2HCO_3^- \quad \text{Eq.1}$$

These anaerobic bacteria gain energy for growth from the oxidation of organic substrates using sulfate as the electron acceptor (Hao et al. 1996, Barton and Tomei 1995). The microbial reduction of sulfate produces hydrogen sulfide and releases of HCO_3^-, resulting in an increase in alkalinity and pH (Richards and Pallud 2016, Mormontoy and Hurtado 2013). After sulfate reduction, sulfide is sequestered by ferrous iron by creating blackish precipitates of pyrite (Boonchayaanant et al. 2010). It was expected that, in the anaerobic conditions, sulfate would be reduced to sulfide and bind to ferrous iron because of the abundance of iron in the SRS sediments. It was also expected that the release of bicarbonate ions, which are produced from the sulfate reduction reaction, would lead to an increase in pH, causing the aqueous phase to become saturated with respect to ferrous carbonate. The research conducted for this subtask can shed light into the limiting factors for the EARP process in an environment such as the one at the F-Area.

METHODOLOGY

Uncontaminated background sediment samples collected from the SRS F-Area from the well FSB 91C, the closest well to the molasses injection site, were selected to conduct the batch experiments. Fine fractions were first separated from SRS sediments through 2 mm, 180 µm, 125 µm and 63 µm sieves in order to remove larger quartz particles. Soil fractioning also helped to decrease the presence of quartz in the samples (suggested by the large intensity peaks shown through X-ray diffraction (XRD) analysis) which overshadows goethite and kaolinite in fine fractions. Before creating any of the samples for the microcosm experiment, XRD analysis was conducted for the 180 µm, 125 µm and 63 µm fractions to obtain a reference for

comparison if any mineralogical changes in the microcosms after sediment treatment with molasses. The sediment composition was predominantly quartz, kaolinite and goethite, which agrees with previous results (Dong et al. 2012a).

The experiment consisted of two batches of microcosm tubes, prepared to mimic conditions at the SRS F-Area. To simulate the anaerobic conditions present in the saturated zone of the SRS F-Area, a vinyl anaerobic airlock chamber was used. The chamber (Coy Lab products) was vacuumed and purged several times with pure nitrogen gas to establish anaerobic conditions, which were then confirmed by the oxygen and hydrogen gas analyzer installed inside the chamber. The glove box environment was continuously monitored to ensure that oxygen level conditions remained anaerobic.

For the first batch, 4 sets of samples were prepared in triplicate for a total of 12 samples. In the second batch, 4 single samples were created due to the low amount of fine fractions collected from the SRS sediments. It should also be noted that Batch 1 was started 42 days prior to Batch 2. In Batch 2, the same basal-molasses solution was used except that the pH was adjusted to a neutral level before the addition of any sediment. All batches followed similar preparation steps and the same types of analysis.

All of the samples for Batches 1 and 2 were prepared in 50-mL polypropylene tubes and were treated using a basal medium solution augmented with sulfate and molasses. The basal medium solution consisted of (in g L^{-1} deionized water): 1.5 $NaHCO_3$, 0.2 NH_4Cl, 0.1 K_2HPO_4 $3H_2O$, 0.055 KH_2PO_4, 0.001 resazurin as a redox indicator, 0.039 Na_2S $9H_2O$ as a sulfur source and reductant, and 0.1 $MgCl_2$ $6H_2O$. In addition, 5 mL L^{-1} trace metal solution was added. The trace metal solution consisted of (in g L^{-1}): 0.005 $FeCl_2$ $4H_2O$, 0.005 $MnCl_2$ $4H_2O$, 0.001 $CoCl_2$ $6H_2O$, 0.0006 H_3BO_3, 0.0001 $ZnCl_2$, 0.0001 $NiCl_2$ $6H_2O$, 0.0001 Na_2MoO_4 $2H_2O$, and 0.002 $CaCl_2$ $2H_2O$ (Freedman and Gossett 1989). Magnesium sulfate anhydrous ($MgSO_4$) salt was used as a source of sulfate for the augmented samples; it was combined with the basal medium solution to a concentration of 500 ppm. The anaerobic process is very slow; to speed up the molasses fermentation process, Sets 1 and 4 were inoculated with 0.5 mL of anaerobic sludge collected from the anaerobic digester of the Miami-Dade South wastewater treatment plant. The complete composition of each tube in Batch 1 and Batch 2 is presented in Table 1.

Table 1. Sample Composition for Batch 1 and Batch 2

Batch 1				
Sample Composition	**Set #1**	**Set #2**	**Set #3**	**Set #4**
Soil, mL	20	20	20	15
Basal Medium, mL	20	20	20	15
Sulfate, ppm	500	500	-	-
Molasses, % by weight	5-10%	5-10%	5-10%	5-10%
Anaerobic sludge, mL	0.5	-	-	0.5
Batch 2				
Soil, mL	20	20	20	15
Basal Medium, mL	12	12	12	12
Sulfate, ppm	500	500	-	-
Molasses, % by weight	5-10%	5-10%	5-10%	5-10%
Anaerobic sludge, mL	0.5	-	-	0.5

Throughout the experiment, all samples underwent a pH evolution study to determine the effects of the additions to the sediments. After the samples were created and given time to react in the anaerobic chamber, sub-samples were taken from both of the microcosm batches to be used for XRD analysis. For Batch 1, a small sub-sample was taken from each of the samples and combined to create a representative sample for each set, with a total of 4 sub-samples. Sub-samples for Batch 1 were taken at week four (4) and week eight (8). For Batch 2, sub-samples were taken directly from each of the tubes for a total of 4 sub-samples. The Batch 2 sub-samples were taken after four (4) weeks in the anaerobic chamber. Each of the dried sub-samples was placed individually onto a plastic sample-holder for the XRD analysis.

XRD analyses were performed using a Bruker 5000D XRD instrument set to 35 kV and 40 mA. Diffraction patterns were obtained using a copper Cu Kα radiation source (λ=0.154056 nm) with a tungsten filter. The XRD was programmed to run over a 2-theta (2θ) range from 3° to 70° with a 0.02° step size and 3 second counting per step. Obtained XRD patterns were analyzed and compared against known XRD patterns for siderite and pyrite minerals.

In addition, inductively coupled plasma optical emission spectrometry (ICP-OES) analysis was conducted on the supernatant solutions to determine the ferrous iron concentrations. Five (5) mL of deionized water (DI) was added to each of the samples and the samples were centrifuged in tubes at 2700 rpm for 20 minutes. The

supernatant was collected from each sample and filtered through a 45 mm filter syringe.

Standards were prepared for iron analysis with a calibration curve between 1 to 100 ppm. The supernatant was collected and diluted by a factor of 200 in 1% nitric acid (HNO_3). Three (3) mL of each of the diluted samples were placed into 15 mL tubes for iron analysis via ICP-OES.

Sulfate analyses were conducted via a Metrohm ion chromatograph equipped with a Metrosep a Supp 5 - 150/4.0 separation IC column. The calibration curve was prepared by using the sulfate standards for 1 ppm, 7 ppm, 17 ppm, 20 ppm and 25 ppm with R^2 of 0.9948. All samples were diluted 20 times before analyses.

Geochemist's Workbench (GWB) 10.0 (Bethke 2007) React Module was used for the geochemical equilibrium modeling to predict the formation of siderite and pyrite solid phases expected to be present as a result of molasses and sulfate additions into the microcosms. This modeling was conducted for an open system with sliding fugacity to 0.1 and simulating CO_2 production during EARP. The synthetic groundwater solutions were formulated using cations and anions concentrations. The experimental conditions were simulated using the React Module, which allowed for varying the Eh to 0.5V at fixed pH value of 4.0, which was observed in the microcosms. This modeling would determine if the EARP process would create a bio-reductive zone in a similar experiment as the Eh is driven down by microbial depletion.

RESULTS AND DISCUSSION

pH Evolution

During the monitoring of the Batch 1 samples, a sharp decrease in the pH from week 1 to week 2 was noted and an investigation was conducted to determine the cause. Previous reports from ARCADIS indicated that the EARP process often results in a decrease in pH (Lutes et al. 2003). It was concluded through an elimination process that the addition of molasses had caused the initial drop in pH. Prior to the molasses addition, the basal media solution with and without sulfate, exhibited more basic pH values ranging between 8.7- 8.8. These values shifted significantly to below pH 5.0 (4.57-4.85) after the molasses addition (Table 2).

Table 2. Measured pH Values

Measured pH values			
Solution amended with sulfate, basal medium and molasses	**Solution amended with basal medium and molasses**	**Basal medium**	**Solution amended with basal medium and 500 ppm of sulfate**
4.85	4.57	8.7	8.82

Due to the pH reduction in the samples of Batch 1, it was decided that a second batch would be prepared with solutions that were first brought to a neutral pH before the addition of the sediments.

The pH measurements suggested that almost all of the samples, in either batch, have followed a similar trend, with a decline in the pH value (Figure 1). This can be attributed to the fermentation process of molasses and the natural acidity of SRS soil used for the microcosm study. It has been found that the fermentative bacteria that thrive in these low pH conditions can out-compete sulfate-reducing and methanogenic bacteria. Lowering of pH to below 5 standard units may inhibit growth of sulfate reducers and methanogens bacteria (Maillacheruvu and Parkin 1996). In addition, the naturally low alkalinity of the SRS soils provides little buffering capacity to the pH changes caused by the molasses. Despite the fact that the fermentative bacteria out-competed the sulfate-reducing bacteria, there was still a slightly higher pH in the sulfate-augmented samples. In general, the pH values for all of the samples inoculated with bacteria were lower than 5 and the difference between sulfate-amended and sulfate-free samples was insignificant.

Both batches received an addition of a small quantity of neutral solution in order to keep the microcosm tubes from drying out. Two solutions were prepared for this purpose for the Batch 2 samples. The first solution consisted of 45 mL of basal medium and 7.1 g molasses. This solution was adjusted to a pH of 7.03 before it was added in the amount of 2 mL per sample to the samples in set 3 and set 4 samples. The second solution consisted of 45 mL of basal medium augmented with 500 ppm of sulfate and 7.1 g molasses. This solution was adjusted to a pH of 6.99 before it was added in the amount of 2 mL per sample to the set 1 and set 2 samples. These additions account for a small increase in the pH evolution graphs at Day 60 for Batch 1 and at Day 18 for Batch 2 (Figure 1). Regardless of initial pH adjustments to neutral, the solutions' pH dropped in all of the Batch 1 and Batch 2 samples. The pH was measured on the level of 4.7 after keeping the samples inside the anaerobic chamber for three weeks and then dropped to 4.0 after keeping the samples inside the chamber for two months (Figure 1).

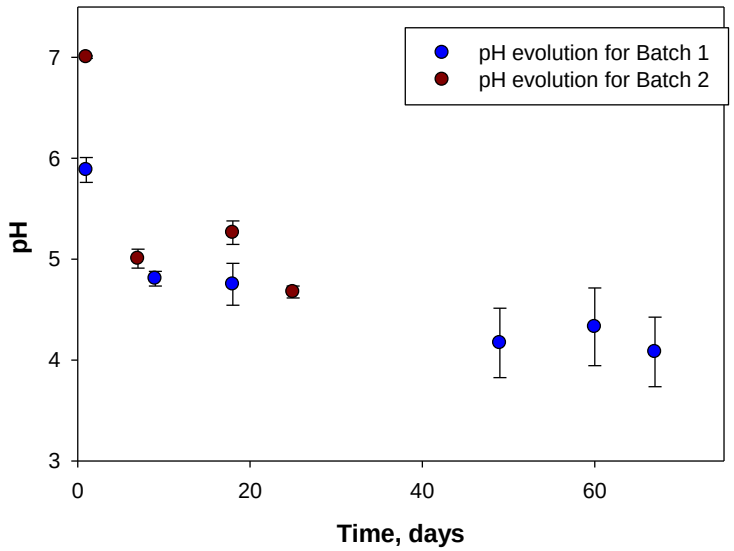

Figure 1. pH evolution for Batch 1 and Batch 2 samples based on measurements of triplicate samples for each set.

X-ray Diffraction Analysis

The initial XRD analyses on the background samples indicated that the sediments contained quartz, kaolinite, montmorillonite, and goethite. The most prominent peak for quartz was observed at 2θ 26.65 degrees, montmorillonite at 5.89 degrees, goethite at 21.37 degrees, and kaolinite at 12.37 degrees (Figure 2-Figure 5). In the molasses treated samples, there were no visible peaks for reduced forms of iron such as siderite and pyrite. The maximum intensity peaks for siderite would occur at 32.49 2-theta value and for pyrite at 28.74 (100%) and 56.75 (84.7%) 2-theta values, respectively. In addition, no evidence of mackinawite at 2-theta 17.62 (100%) or ankerite at 30.83 (100%) was observed (Figure 6, Figure 7). Due to the fact that no matches to siderite or pyrite were found in any sample, only a few of the XRD graphs have been displayed. All samples in both batches displayed nearly identical XRD patterns when compared against XRD results of the background sediment before beginning the microcosm experiment.

SRS soil is very low in the carbonate alkalinity needed for the formation of ferrous carbonate and the acidic pH of the samples might play a role in the lack of ferrous iron solid phases formation.

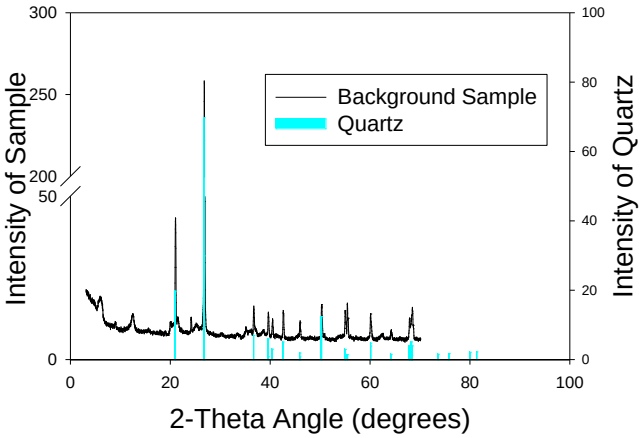

Figure 2. Background sample vs. quartz.

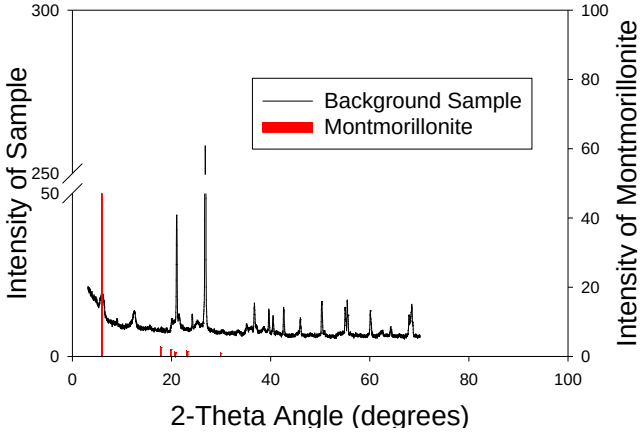

Figure 3. Background sample vs. montmorillonite.

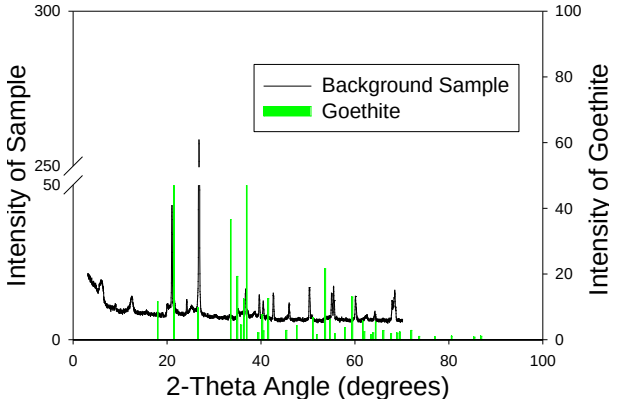

Figure 4. Background sample vs. goethite.

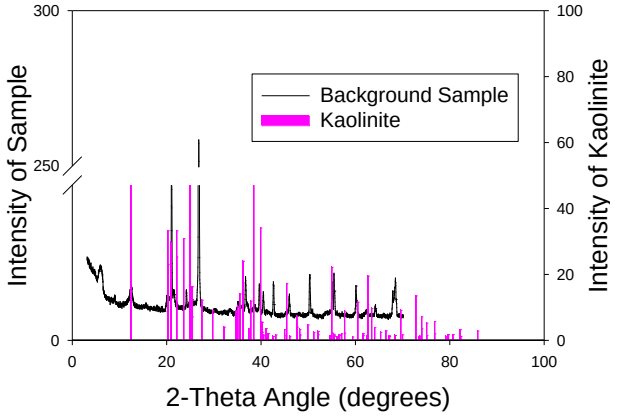

Figure 5. Background sample vs. kaolinite.

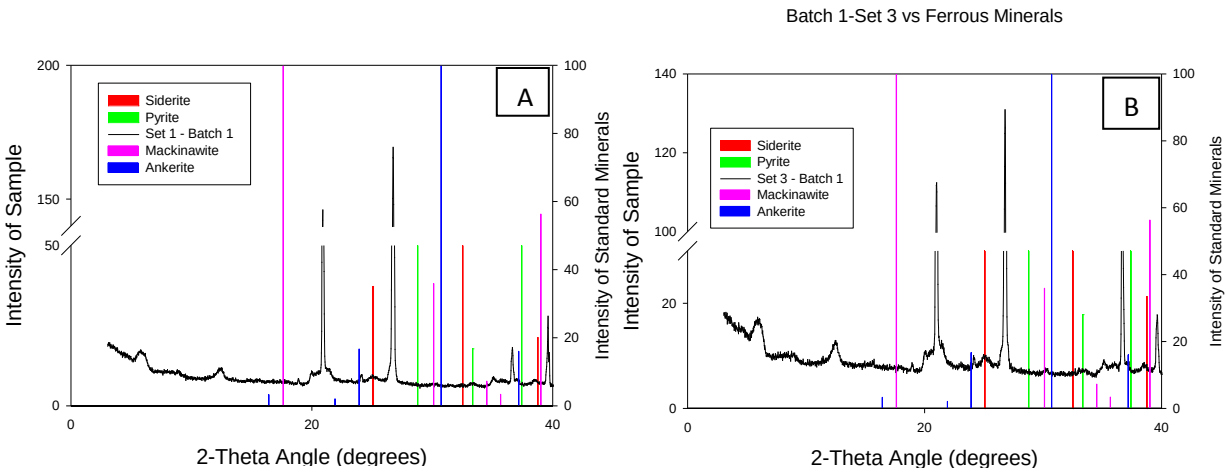

Figure 6 XRD data to identify ferrous minerals in Batch 1 samples treated with molasses; A) Set 1; B) Set 3. No matches were found to ferrous iron minerals in any of samples.

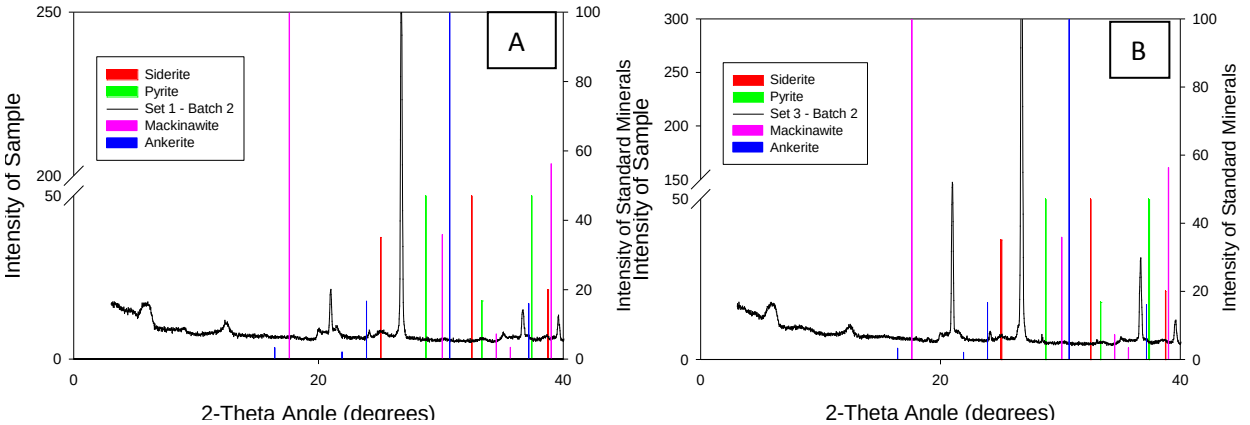

Figure 7 XRD data to identify ferrous minerals in Batch 2 samples treated with molasses; A) Set 1; B) Set 3. No matches to ferrous iron minerals were found in any of samples.

Samples Analysis for Sulfate and Iron

In the acidic iron-rich sediments, the microbial reduction of Fe(III) is the dominant electron-accepting process for the oxidation of organic matter (Küsel 2003). Potential Fe(III) reduction was measured by the accumulation of Fe(II) during incubation in an anaerobic glove box. Iron analyses of the supernatant solutions extracted from the samples were conducted via ICP-OES. The samples varied significantly in iron concentration, with the greatest reaching 7808 µg/L in Batch 1/Set 1 samples. It was found that the samples amended with sulfate (Sets 1 and 2) did not display a significant difference in average iron concentration in comparison to the samples which contained no sulfate, 5726.54 µg/L vs. 4907.53 µg/L, respectively. This suggests that the ferrous iron most likely doesn't complex with sulfide ions to create pyrite solid phase due to the hindering of sulfate reduction in the acidic conditions. The variation in iron concentrations is most probably due to slight differences in the soil composition upon preparation of the microcosm tubes.

It was also noted that the Batch 1 samples containing anaerobic bacteria (Sets 1 and 4) had higher average iron concentrations in comparison to those which were not inoculated. It is believed that the samples inoculated with anaerobic sludge contain an adequate amount of active iron-reducing bacteria that may have biodegraded the molasses using ferric iron as a terminal electron acceptor, leading to the higher concentrations of soluble ferrous iron in these samples.

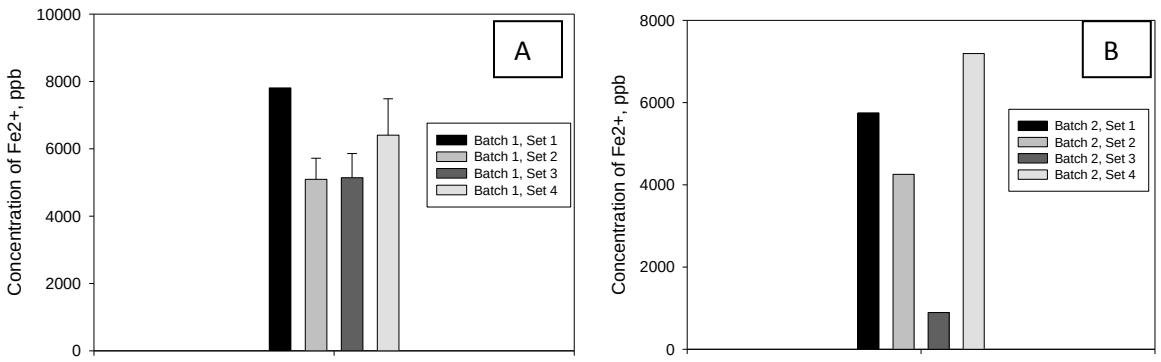

Figure 8. Iron concentrations detected in supernatant solutions of (A) Batch 1 and (B) Batch 2 samples.

Sulfate analyses were conducted via ion chromatography for the liquid samples collected from the microcosm experiments. All samples collected for analysis were kept under anaerobic conditions in the anaerobic glove box until time of assay. A calibration curve was prepared by using a sulfate standard in the concentration range from 1 ppm to 25 ppm (Figure 9).

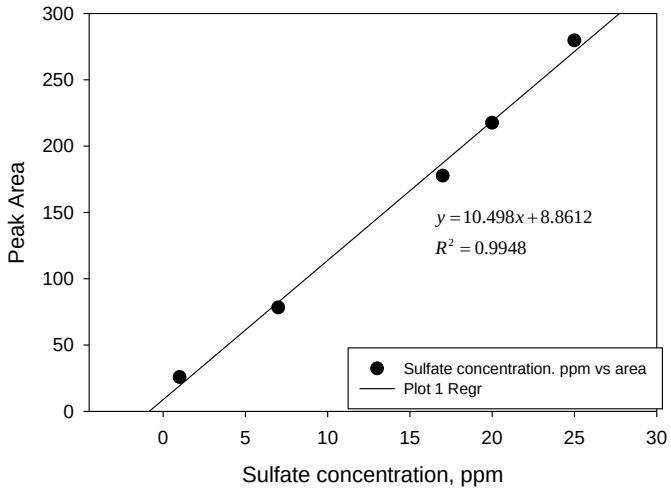

Figure 9. Calibration curve for sulfate analysis.

Analytical results showed that there was no sulfate reduction in any of samples augmented with sulfate and the concentration remained on the level of 500 ppm as originally added to the initial solutions (518-542±14.5 ppm). The lack of sulfate reduction explains why no iron sulfide phases were observed. Literature suggests that SRB microorganisms are very adaptable to many environmental conditions, including acid mine drainages and acidic sediments (Costa and Duarte 2005, Muyzer and Stams 2008, Fauque and Ollivier 2004, Hussain et al. 2016). Meier et al. (2004) reported that sulfate reduction rates were much lower in the slightly acidic sediment than in the pH-neutral sediment because of reduced microbial activity (Meier et al. 2004). Moreover, in the zone of ferric iron reduction in sediments, sulfate reduction is a competitive mechanism, leading to the inhibition of sulfate reduction on the level

of 86% to 100% (Lovley and Phillips 1987). Literature data demonstrated that Fe(III)-reducing bacteria can outcompete sulfate-reducing food chains for organic matter in acidic sediment (Peine et al. 2000). Fe(III) phases don't have a direct toxic effect on sulfate-reducing bacteria and the inhibition of sulfate reduction is more a result of organic substrate limitation (Lovley and Phillips 1987). Apparently, if electron donors are not limiting the iron and sulfate reduction processes, they can take place simultaneously. Iron in SRS sediments is present as oxide minerals that exist as a coating on clay and quartz minerals surfaces. The abundance of biologically available Fe(III) allows Fe(III) reducers to outcompete sulfate-reducing bacteria using molasses as an electron donor.

Speciation Modeling

Speciation modeling was conducted via Geochemists Workbench (GWB) software. Aqueous speciation and saturation indices of solid phases are presented in **Error! Reference source not found.**. Iron is mostly present as soluble ferrous iron ions.

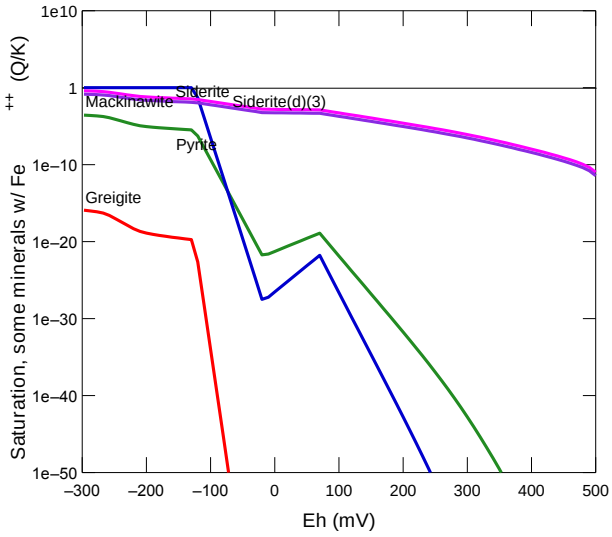

Figure 10. GWB simulations conducted for conditions mimicking the enhanced anaerobic reductive precipitation (EARP) remediation method previously tested at SRS F- Area.

Speciation modeling suggested the formation of siderite is close to saturation at pH4 and very low Eh (–300 mV). Modeling also predicted the formation of iron sulfide minerals (pyrite and mackinawite); however, they became unsaturated at an Eh of -100 mV. A ferrous sulfate solid phase (melanterite) was predicted to be near saturation from an Eh of -200 to 500 mV. The speciation modeling predicted that as the Eh is driven down by the sulfate microbial reduction, the potential formation of siderite and iron sulfide is thermodynamically favorable. Authors haven't observed the formation of these minerals via XRD analysis with a reduction of sulfate, but did note a reduction of iron, which is consistent with the hypothesis of this manuscript.

CONCLUSION

Microcosm experiments were performed to investigate the addition of molasses to create anaerobic conditions in the acidic SRS sediments collected from the F-Area. In

the anaerobic conditions, microbially-mediated Fe(III) reduction resulted in an increase of ferrous iron concentration that in the acidic conditions is mostly present in solutions as soluble Fe^{2+} ions. These conditions open up the potential for reduction of highly mobile uranyl (UVI) ions to insoluble reduced U(IV) phases. This process of uranyl reduction can be catalyzed by ferrous iron (Liger et al. 1999, Boland et al. 2011, Tsarev et al. 2016) over a limited pH range, which could result in the immobilization of uranium. However, if no mineralogical changes occur in the acidic soil forming ferrous iron minerals due to the addition of molasses, soluble ferrous iron can be oxidized to ferric iron as molasses is rapidly fermented or flushed out from the treatment zone with groundwater. This would affect the stability of the reduced uranium species and lead to their re-oxidation to highly soluble and mobile uranyl ions.

REFERENCES

Annachhatre, A. P. & S. Suktrakoolvait (2001) Biological sulfate reduction using molasses as a carbon source. *Water Environment Research,* 73**,** 118-126.

Aravena, R. & B. Mayer (2009) Isotopes and processes in the nitrogen and sulfur cycles. *Environmental isotopes in biodegradation and bioremediation***,** 203-246.

Barton, L. L. & F. A. Tomei. 1995. Characteristics and activities of sulfate-reducing bacteria. In *Sulfate-reducing bacteria*, 1-32. Springer.

Berner, Z. A., D. Stüben, M. A. Leosson & H. Klinge (2002) S-and O-isotopic character of dissolved sulphate in the cover rock aquifers of a Zechstein salt dome. *Applied geochemistry,* 17**,** 1515-1528.

Bethke, C. M. 2007. *Geochemical and biogeochemical reaction modeling*. Cambridge University Press.

Boland, D. D., R. N. Collins, T. E. Payne & T. D. Waite (2011) Effect of amorphous Fe (III) oxide transformation on the Fe (II)-mediated reduction of U (VI). *Environmental science & technology,* 45**,** 1327-1333.

Boonchayaanant, B., B. H. Gu, W. Wang, M. E. Ortiz & C. S. Criddle (2010) Can microbially-generated hydrogen sulfide account for the rates of U(VI) reduction by a sulfate-reducing bacterium? *Biodegradation,* 21**,** 81-95.

Canfield, D. E. (2001) Isotope fractionation by natural populations of sulfate-reducing bacteria. *Geochimica et Cosmochimica Acta,* 65**,** 1117-1124.

Costa, M. & J. Duarte (2005) Bioremediation of acid mine drainage using acidic soil and organic wastes for promoting sulphate-reducing bacteria activity on a column reactor. *Water, air, and soil pollution,* 165**,** 325-345.

Dennis, E. & A. G. Suthersan. 1998. Microbial Precipitation of Dissolved Metals Using Molasses. EPA 542-N-98-010.

Dong, W., T. K. Tokunaga, J. A. Davis & J. Wan (2012a) Uranium (VI) adsorption and surface complexation modeling onto background sediments from the F-Area Savannah River Site. *Environmental science & technology,* 46**,** 1565-1571.

Dong, W., T. K. Tokunaga, J. A. Davis & J. Wan (2012b) Uranium(VI) Adsorption and Surface Complexation Modeling onto Background Sediments from the F-Area Savannah River Site. *Environmental Science & Technology,* 46**,** 1565-1571.

Fauque, G. & B. Ollivier (2004) Anaerobes: the sulfate-Reducing Bacteria as an Example of Metbolic Diversity. *Microbial Diversity and Bioprospecting,* 17**,** 169-176.

Freedman, D. L. & J. M. Gossett (1989) Biological reductive dechlorination of tetrachloroethylene and trichloroethylene to ethylene under methanogenic conditions. *Applied and Environmental Microbiology,* 55**,** 2144-2151.

Hao, O. J., J. M. Chen, L. Huang & R. L. Buglass (1996) Sulfate-reducing bacteria. *Critical reviews in environmental science and technology,* 26**,** 155-187.

Hussain, A., A. Hasan, A. Javid & J. I. Qazi (2016) Exploited application of sulfate-reducing bacteria for concomitant treatment of metallic and non-metallic wastes: a mini review. *3 Biotech,* 6**,** 1-10.

Hussain, A., J. I. Qazi & H. A. Shakir (2014) Implication of molasses as electron donor for biological sulphate reduction. *American Journal of Environmental Engineering,* 4**,** 7-10.

Küsel, K. (2003) Microbial cycling of iron and sulfur in acidic coal mining lake sediments. *Water, Air and Soil Pollution: Focus,* 3**,** 67-90.

Liger, E., L. Charlet & P. Van Cappellen (1999) Surface catalysis of uranium (VI) reduction by iron (II). *Geochimica et Cosmochimica Acta,* 63**,** 2939-2955.

Lovley, D. R. & E. J. Phillips (1987) Competitive mechanisms for inhibition of sulfate reduction and methane production in the zone of ferric iron reduction in sediments. *Applied and Environmental Microbiology,* 53**,** 2636-2641.

Lutes, C. C., P. Angela Frizzell, T. A. Thornton & J. M. Harrington. 2003. *In-situ* chemical stabilization of metals and radionuclides through enhanced anaerobic reductive precipitation. Arcadis Geraghty & Miller, Inc.(US).

Lutes, C., A. Frizzell, J. Gillow, & J. Beckner (2014) In Situ Precipitation of Radionuclides in Groundwater at US DOE Savannah River Site. Proceedings Waste Management Conference 2014, Phoenix AZ.

Maillacheruvu, K. Y. & G. F. Parkin (1996) Kinetics of growth, substrate utilization and sulfide toxicity for propionate, acetate, and hydrogen utilizers in anaerobic systems. *Water Environment Research,* 68**,** 1099-1106.

Meier, J., H.-D. Babenzien & K. Wendt-Potthoff (2004) Microbial cycling of iron and sulfur in sediments of acidic and pH-neutral mining lakes in Lusatia (Brandenburg, Germany). *Biogeochemistry,* 67**,** 135-156.

Mormontoy, J. & J. E. Hurtado. 2013. Hydrogen sulphide production at alkaline, neutral and acid pH by a bacterial consortium isolated from Peruvian mine tailing and wetland. In *Integration of Scientific and Industrial Knowledge on Biohydrometallurgy,* eds. N. Guiliani, C. Demergasso, R. Quatrini, F. Remonsellez, C. DavisBelmar, G. Levican, P. Parada, C. Barahona & R. Zale, 384-387. Stafa-Zurich: Trans Tech Publications Ltd.

Muyzer, G. & A. J. Stams (2008) The ecology and biotechnology of sulphate-reducing bacteria. *Nature Reviews Microbiology,* 6**,** 441-454.

Peine, A., A. Tritschler, K. Küsel & S. Peiffer (2000) Electron flow in an iron-rich acidic sediment—evidence for an acidity-driven iron cycle. *Limnology and Oceanography,* 45**,** 1077-1087.

Richards, C. M. & C. Pallud (2016) Kinetics of sulfate reduction and sulfide precipitation rates in sediments of a bar-built estuary (Pescadero, California). *Water Research,* 94**,** 86-102.

Tsarev, S., T. D. Waite & R. N. Collins (2016) Uranium reduction by Fe (II) in the presence of montmorillonite and nontronite. *Environmental Science & Technology*.

Willis, L. C., H. J. Cummings, G. Neale & R. G. Gibson (1997) Nutritional Aspects of Dissimilatory Sulfate Reduction in the Human Large Intestine. *Current Microbiology,* 35**,** 294-298.

ACKNOWLEDGEMENTS

Funding for this research was provided by U.S. DOE cooperative agreement number DE-EM0000598. We truly appreciate Dr. Brian Looney from SRNL for his support of this research. XRD analyses were conducted at FIU AMERI facilities.